

## Article

# Effect of Nano-Silver Solution Microcapsules Mixed with Rosin-Modified Shellac Microcapsules on the Performance of Water-Based Coating on Andoung Wood (*Monopetalanthus* spp.)

Yuming Zou <sup>1,2</sup>, Pan Pan <sup>1,2</sup>, Nana Zhang <sup>1,2</sup> and Xiaoxing Yan <sup>1,2,\*</sup>

<sup>1</sup> Co-Innovation Center of Efficient Processing and Utilization of Forest Resources, Nanjing Forestry University, Nanjing 210037, China; zou\_yuming@njfu.edu.cn (Y.Z.); pan@njfu.edu.cn (P.P.); znn@njfu.edu.cn (N.Z.)

<sup>2</sup> College of Furnishings and Industrial Design, Nanjing Forestry University, Nanjing 210037, China

\* Correspondence: yanxiaoxing@njfu.edu.cn

**Abstract:** To obtain dual functions of antibacterial and self-healing of a coating, nano-silver solution microcapsules coated with urea formaldehyde resin were selected for antibacterial agents, and rosin-modified shellac microcapsules coated with melamine formaldehyde resin were selected for repairing agents. The optical, mechanical, antibacterial, self-healing, and other physicochemical properties of the coatings were analyzed. The method of adding two microcapsules independently did not affect the coating's hardness. When the primer was prepared by self-healing microcapsules and the topcoats were prepared by antibacterial microcapsules, the hardness of the prepared coatings was maintained at 3 H, with the adhesion up to class 2, the impact strength up to 18 kg·cm, and the roughness as low as 1.144 μm. The elongation at fracture of the coatings prepared by adding microcapsules independently was improved by 2.2%. The self-healing microcapsules release the repair agents to improve the mechanical properties of the coatings. In terms of the antibacterial properties of the coatings, the method that involves adding the microcapsules independently is better than mixed adding. Against *Escherichia coli*, the antibacterial rate of coatings prepared by adding microcapsules independently reached 82%. Against *Staphylococcus aureus*, the antibacterial rate of coatings reached 83.3%. At the same time, the self-healing rate was up to 41.1%. The two microcapsules were added to the water-based coating independently to obtain antibacterial and self-healing functions with good comprehensive properties. By modifying coatings on the Andoung wood (*Monopetalanthus* spp.) with antibacterial microcapsules and self-healing microcapsules, it is possible to obtain good antibacterial properties, further protect the wood substrate, and broaden the application range of functional coatings.

**Keywords:** microencapsulation; rosin-modified shellac microcapsules; antibacterial properties; self-healing properties



**Citation:** Zou, Y.; Pan, P.; Zhang, N.; Yan, X. Effect of Nano-Silver Solution Microcapsules Mixed with Rosin-Modified Shellac Microcapsules on the Performance of Water-Based Coating on Andoung Wood (*Monopetalanthus* spp.). *Coatings* **2024**, *14*, 286. <https://doi.org/10.3390/coatings14030286>

Academic Editors: Gabriela Olimpia Isopencu and Alexandra Mocanu

Received: 29 December 2023

Revised: 21 February 2024

Accepted: 23 February 2024

Published: 27 February 2024



**Copyright:** © 2024 by the authors. Licensee MDPI, Basel, Switzerland. This article is an open access article distributed under the terms and conditions of the Creative Commons Attribution (CC BY) license (<https://creativecommons.org/licenses/by/4.0/>).

## 1. Introduction

Wood is a natural renewable material [1]. With a warm feel and beautiful pattern, wood is widely used in the furniture industry [2–5]. Given a characterization of dry shrinkage and wet expansion, as well as the impact of environmental factors, the surface of wooden furniture often cracks. This phenomenon will reduce the service life of furniture [6,7]. Therefore, to improve the service life of the wooden furniture, people began to add a coating to the surface of the furniture to protect it [8,9]. Water-based coatings are widely used nowadays because of their advantages, such as the fast drying speed, environmental protection, and pollution resistance [10,11]. With the application of water-based coatings, it was found that the water-based coating has some defects. For example, after application for the long term, the coating on the surface of wooden furniture will be affected by moisture and other factors in the environment [12]. These factors will make coating properties decrease because of micro-cracks. If the micro-cracks cannot be repaired in time, they

will expand and fracture the coating structure, which will negatively affect the feelings of the furniture users and reduce the service life of the furniture [13]. The wood can easily breed bacteria and does not have antibacterial activity. The water-based coatings do not have antibacterial properties, either. Therefore, with people's attention to health, the development of water-based coatings with antibacterial and self-healing properties on the wood surface has broad prospects.

The reason why silver can inhibit bacteria is because most of the bacteria are unicellular microorganisms that rely on proteases to maintain metabolism. When silver encounters proteases, the activity of proteases will take away an electron of silver, making silver atoms into silver particles. The silver particles will effectively puncture the cell membrane. They can also further make the bacteria unable to breathe, metabolize, and reproduce due to protein denaturation until the bacteria die. Thus, they achieve the effect of inhibiting bacteria. With the increasing resistance of bacteria to existing antibiotics and the steady advancement of nanoscience, there has been renewed interest in the study of silver and its compounds [14]. Nano-silver particles were widely used in biomedical fields, especially in the antibacterial field [15,16].

Nano-silver particles refer to elemental silver particles with particle sizes ranging from 1 to 100 nm obtained by chemical or physical methods. Compared with ordinary silver particles, nano-silver had better chemical reactivity, biological activity, and catalytic properties [17]. Silver-based antibacterial materials have been used by humans for many years because they can effectively kill bacteria. In the 1960s, Moyer believed that 0.5% silver nitrate solution would not interfere with epidermal cell proliferation but did have obvious antibacterial effects on *Staphylococcus aureus*, *Hemolytic streptococcus*, *Pseudomonas aeruginosa*, and *Escherichia coli* [18]. Nano-silver particles have been favored by researchers because of their broad-spectrum antibacterial activity and their lower resistance [19]. Researchers have worked on developing various methods of preparing nano-silver particles, such as chemical reduction and physical methods, and characterizing them in detail via different techniques. Haidari et al. first prepared nano-silver particles using sodium borohydride as a reducing agent and mercaptosuccinic acid as a stabilizing agent [20]. Huang et al. successfully prepared a silver-containing composite system (PM-Ag-Cur) by using biodegradable polymer micelles as nanocarriers, modifying nano-silver particles on polymers, and encapsulating curcumin in the core [21]. Nano-silver particles perform well in antibacterial applications, effectively disrupting the bacteria and inhibiting their growth. In recent years, with the rapid development of nanotechnology, nano-silver particles have been widely used in medical treatment and daily life because of their stronger antibacterial properties and lower resistance [22]. However, the stability and reproducibility of nano-silver particles still need to be improved. Therefore, researchers have improved the antibacterial properties and stability of nano-silver particles by adjusting the size, shape, and composition of nano-silver particles, as well as optimizing the preparation method of nano-silver particles. Nogueira et al. successfully prepared nano-silver particles by using sodium borohydride as a reducing agent and diamino silane as a stabilizing agent and used them in antibacterial research. The nano-silver particles were proven to have good antibacterial properties against *Staphylococcus aureus* [23]. The antibacterial property of nano-silver particles is mainly based on their unique surface reaction process, and the property enables nano-silver particles to interact effectively with bacterial cells. The nano-silver particles form an antibacterial layer and cause the proteins in bacteria to coagulate, achieving an antibacterial property. Nano-silver particles have significant antibacterial ability against *Escherichia coli* and *Staphylococcus aureus*, among others. Nano-silver particles can be prepared from leaf extracts of *Catharanthus roseus* and *Azadirachta indica* in a very environmentally friendly way. Moreover, nano-silver particles are effective in inhibiting the growth of multidrug-resistant bacteria [24].

The clustering of nano-silver particles reduces their opportunity of uptake into biological systems. The stability of nano-silver particles has been shown to be a crucial factor for their long-term antibacterial durability. The nature of the capping agent affects the size and appearance of the nano-silver particles and their interaction with the solvent [25]. An appropriate capping agent is beneficial to the stability of the antibacterial property of nano-silver particles.

Microcapsules refer to the use of polymer materials such as solid, solution, and gas encapsulation into tiny particles. The existence mode of the core material mainly includes an emulsion, dispersion, or solution form. The microcapsule wall acts as a barrier to protect the core material from the external environment. There were many kinds of microcapsules studied by researchers. At the beginning of the 21st century, White's group in the United States took the lead in proposing the self-healing method of microcapsules, and the United States has become a hotspot of research in the field of material science [26]. In 1949, the mechanical preparation method of microcapsules independently developed by Wurster at the University of Wisconsin was widely used in the medical field. Rodrigues et al. produced polyurethane/urea (PUU) microcapsules with fragrances for industrial applications in textile substrates [27]. Xu et al. used two kinds of biopolymers as wall materials to enhance the effect of sunscreen on octyl methoxycinnamate microcapsules [28]. In addition, azobenzene-containing layer-by-layer self-assembled membranes (LbL) and microcapsules have been used as carriers for light-sensitive drug delivery systems. UV irradiation was able to trigger changes in the permeability of LbL and the breakdown of microcapsules, resulting in the release of encapsulated drugs and proteins. This means that the fast response time, high healing efficiency, and excellent antibacterial properties of the dual-functional coatings have potential application value [29]. This will be the general direction and research path of current scientific research, making materials dual-functional and intelligent. The purpose of this study was to prepare microcapsules by coating nano-silver solution and applying them to a wood surface mixed with self-healing microcapsules. Under the premise of keeping the properties of the original water-based coating unchanged, coatings had the dual functions of antibacterial and self-healing activity.

In this paper, antibacterial microcapsule-coated nano-silver solutions were mixed with self-healing microcapsules. Orthogonal experiments were designed with the content of self-healing microcapsules and microcapsule adding methods and the coating methods as influencing factors to obtain the best adding method. After coating the Andoung wood (*Monopetalanthus* spp.) with the water-based coating prepared with microcapsules, the optical, mechanical, resistance-to-liquid, antibacterial, and self-healing properties of the coatings were investigated. The results provide a reference for applications of antibacterial microcapsules in water-based coatings.

## 2. Materials and Methods

### 2.1. Materials of Test

The transparent shellac for the preparation of self-healing microcapsules was supplied by Jinan Yongtai Chemical Co. Ltd., Jinan, China. The rosin solution was supplied by Linyi Dongye Trading Co. Ltd., Linyi, China. The Andoung wood was supplied by the laboratory, with the specification of 50 mm × 100 mm × 5 mm. Table 1 is the list of experimental materials information. The nano-silver particle content is 25 PPM in the transparent nano-silver solution, with a particle size of 5–7 nm.

**Table 1.** List of experimental materials information.

Materials	Materials Firm
Nano-silver solution (25 PPM)	Tianjin Beichen Founder Reagent Factory, Tianjin, China
37.0% formaldehyde	Xi'an Tianmao Chemical Co., Ltd., Xi'an, China
Melamine C <sub>3</sub> H <sub>6</sub> N <sub>6</sub>	Shandong Zibo Haijie Chemical Co., Ltd., Zibo, China
Triethanolamine	Guangzhou Jiale Chemical Co., Ltd., Guangzhou, China
Tween-80 (emulsifier)	Wuxi Yatai United Chemical Co., Ltd., Wuxi, China
Tween-20 (emulsifier)	Wuxi Yatai United Chemical Co., Ltd., Wuxi, China
Span-80 (emulsifier)	Shandong Zibo Haijie Chemical Co., Ltd., Zibo, China
Citric acid monohydrate	Nanjing Quanlong Biotechnology Co., Ltd., Nanjing, China
Absolute ethanol	Guangzhou Kema Chemical Technology Co., Ltd., Guangzhou, China
Acetic acid (CH <sub>3</sub> COOH)	Shanghai Sinopharm Chemical Reagent Co., Ltd., Shanghai, China
Water-based primer	Akzo Nobel Paint Co., Ltd., Guangzhou, China
Water-based topcoat	Akzo Nobel Paint Co., Ltd., Guangzhou, China
<i>Escherichia coli</i>	Beijing Conservation Biotechnology Co., Ltd., Beijing, China
<i>Staphylococcus aureus</i>	Beijing Conservation Biotechnology Co., Ltd., Beijing, China
Nutrient agar	Qingdao Hope Bio-Technology Co., Ltd., Qingdao, China
Nutritious broth	Chixing Pharmaceutical Technology Co., Ltd., Hangzhou, China
Detergent	Sichuan Kelun Pharmaceutical Co., Ltd., Chengdu, China
Red ink	Guangzhou Hero Hailuo Cultural Products Co., Ltd., Guangzhou, China
Ethanol (medical grade)	Shandong Elimokang Medical Supplies Co., Ltd., Shandong, China

### 2.2. Preparation of Nano-Silver Solution Microcapsules

The preparation method of nano-silver solution microcapsules was developed from previous studies [30].

- (1) Urea–formaldehyde prepolymer (the wall materials): A total of 7.0 g of urea was weighed and added to a beaker. Then, 9.47 g of formaldehyde was added. The ratio of urea and formaldehyde was determined according to the 1:1 molar ratio. A magnetic rotor was added into the beaker which was in the water bath. While two materials were stirred thoroughly to mix them uniformly, the temperature of the water bath was formulated to 70 °C. The rotation speed of the water bath was adjusted to 600 rpm. At this time, the solution was added dropwise by 2 mL of triethanolamine to adjust the pH value to 8–9. The mouth of the beaker was sealed with a layer of plastic wrap to protect the solution from oxidation. After the solution was maintained colorless and transparent for about 30 min, it was cooled at room temperature.
- (2) Nano-silver solution (the core materials): First, 8.4 g of nano-silver solution was added. Ethanol, Span-80, and Tween-80 were weighed in quantity and stirred with a glass rod until the Span-80 and Tween-80 dissolved. An emulsifier with a concentration of about 2% was obtained. The emulsifier was added dropwise to the nano-silver solution. The temperature of the water bath was controlled at 60 °C, and the rotation speed was controlled at 600 rpm. The emulsion of core materials was obtained after emulsification for 1 h.
- (3) Microcapsules: The rotation speed of the water bath was kept at 600 rpm. The urea–formaldehyde prepolymer was slowly and gradually added to the emulsion of core material with a pipette. The 8% citric acid monohydrate was added to adjust the pH value to about 2.5–3.0. Then, they reacted for 3 h under the water bath and then stood still. After 3 days of cooling at room temperature, the wall material, core material, and remaining emulsion were washed repeatedly with distilled water and ethanol in a vacuum filter. The filter paper was removed after vacuum filtration when the water after washing became transparent. The microcapsules were then poured into petri dishes. The powdered microcapsules were obtained after drying for 48 h. The oven was formulated at 60 °C.

### 2.3. Preparation of Self-Healing Microcapsules

The microcapsules were prepared by in situ polymerization.

- (1) Preparation of melamine–formaldehyde prepolymer (the wall materials): The melamine–formaldehyde resin, the wall materials, were prepared, and they were formulated in a molar ratio of 3.5:1. A mixture of wall materials was stirred at 800 rpm, and the pH value of the mixture was adjusted to the range of 8.0–9.0 by adding triethanolamine dropwise. The mixture was stirred slowly, using the magnetic rotor. The temperature of the water bath was raised to 70 °C. The solution was stirred for 30 min at 800 rpm. Then the melamine–formaldehyde prepolymer was obtained.
- (2) Preparation of a rosin-modified shellac (the core materials): A total of 4.4 g of rosin solution and the 4.4 g of shellac were weighed and mixed for use. Then, 78.9 mL of ethanol, 0.15 g of Span-20, and 0.15 g of Tween-20 were compounded to prepare an emulsifier with a concentration of 1%. The emulsifier was added dropwise to the mixture of rosin and shellac and then transferred to a water bath. The system was stirred for 1 h to obtain the core solution.
- (3) Preparation of melamine–formaldehyde resin-coated rosin-modified shellac microcapsules: The wall material was added dropwise to the core solution, dispersed with an ultrasonic disperser for 15 min, and then transferred to a water bath. The pH value of the solution was adjusted to 4 with citric acid monohydrate solution. The stirring rotation speed of the reaction was controlled at 600 rpm for 3 h at 60 °C. At the end of the process, it was put in the oven for 3 days. Then, the products were washed repeatedly with distilled water and ethanol, filtered several times, and then dried in the oven at 60 °C for 2 days to obtain a white powder that was the self-healing microcapsules.

#### 2.4. Preparation of Coatings with Antibacterial Microcapsules Mixed with Self-Healing Microcapsules

From the previous studies, when the nano-silver solution microcapsules were formulated with  $W_{\text{core}}/W_{\text{emulsion}}$  of 1:4,  $W_{\text{core}}/W_{\text{wall}}$  of 0.8:1 and a rotation speed of 1000 rpm, the coatings prepared by the content of microcapsules was 5% and had optimal comprehensive properties, such as antibacterial properties [31]. With 3-factor and 2-level orthogonal tests (Table 2), the 4 groups of tests were designed by mixing self-healing microcapsules and antibacterial microcapsules. The specific tests are shown in Table 3. The content of self-healing microcapsules, mixing or independent adding methods, and coating methods were taken as the factors. Among them, two adding methods were selected. One was that primers were a pure water-based coating, while topcoats were coated with self-healing microcapsules and antibacterial microcapsules as mixing adding method A to investigate the effect of the mixing adding method on self-healing and antibacterial properties of coatings. The independent adding method B was that each layer of coatings was prepared by different types of microcapsules to investigate the self-healing properties and antibacterial properties of the coatings when two types of microcapsules were added independently. The two coating methods of 1 primer with 2 topcoats and 3 primers with 2 topcoats were commonly used in furniture enterprises. By compositing these adding methods, the effect of the adding methods on the performance of coatings was investigated. The antibacterial properties of coatings applied on the Andoung wood were used as test results to compare the 4 groups of tests.

**Table 2.** The 3-factor and 2-level orthogonal tests.

Levels	Content of Self-Healing Microcapsules (%)	Adding Method	Coating Method
1	3	Mixing adding method A	1 primer/2 topcoats
2	6	Independent adding method B	3 primers/2 topcoats

Table 3. Tests' arrangements.

Samples (#)	Content of Self-Healing Microcapsules (%)	Adding Method	Coating Method
1	3	Mixing adding method A	1 primer/2 topcoats
2	3	Independent adding method B	3 primers/2 topcoats
3	6	Mixing adding method A	3 primers/2 topcoats
4	6	Independent adding method B	1 primer/2 topcoats

A maximum influencing factor was obtained to design single-factor tests to obtain optimal process parameters for coatings prepared with microcapsules. Table 4 shows the single-factor tests, where “primer” is abbreviated as “P”, “topcoat” is abbreviated as “T”, “self-healing microcapsules” is abbreviated as “s”, and “antibacterial microcapsules” is abbreviated as “a”, respectively.

Table 4. Single-factor tests.

Samples (#)	Types	Adding Methods	Antibacterial Microcapsules (g)	Self-Healing Microcapsules (g)	Primer (g)	Topcoat (g)
1	A	P <sub>sa</sub> T	0.050	0.060	0.890	1.000
2	A	PT <sub>1sa</sub>	0.025	0.030	1.000	0.945
3	A	PT <sub>2sa</sub>	0.025	0.030	1.000	0.945
4	B	P <sub>a</sub> T <sub>1s</sub>	0.050	0.030	0.950	0.970
5	B	P <sub>a</sub> T <sub>2s</sub>	0.050	0.030	0.950	0.970
6	B	P <sub>s</sub> T <sub>1a</sub>	0.060	0.025	0.940	0.975
7	B	P <sub>s</sub> T <sub>2a</sub>	0.060	0.025	0.940	0.975
8	B	PT <sub>1a2s</sub>	0.025	0.030	1.000	0.945
9	B	PT <sub>2a1s</sub>	0.025	0.030	1.000	0.945

In Table 4, sample 1# (P<sub>sa</sub>T) was created via a mixing adding method wherein the self-healing and antibacterial microcapsules were mixed in the primer, and the topcoat was the water-based coating. Sample 2# (PT<sub>1sa</sub>) was created via a mixing adding method that the primer was the water-based coating, and the self-healing and antibacterial microcapsules were mixed in the first topcoat. Sample 3# (PT<sub>2sa</sub>) was made via a mixing adding method in which the primer was the water-based coating, and the self-healing and antibacterial microcapsules were mixed in the second topcoat. Sample 4# (P<sub>a</sub>T<sub>1s</sub>) was made via an independent adding method in which antibacterial microcapsules were added to the primer, and self-healing microcapsules were added to the first topcoat. Sample 5# (P<sub>a</sub>T<sub>2s</sub>) was created through an independent adding method in which the antibacterial microcapsules were added to the primer, and the self-healing microcapsules were added to the second topcoat. Sample 6# (P<sub>s</sub>T<sub>1a</sub>) was created through an independent adding method in which the self-healing microcapsules were added to the primer, and the antibacterial microcapsules were added to the first topcoat. Sample 7# (P<sub>s</sub>T<sub>2a</sub>) was created through an independent adding method in which the self-healing microcapsules were added to the primer, and the antibacterial microcapsules were added to the second topcoat. Sample 8# (PT<sub>1a2s</sub>) was created through an independent adding method in which the primer was the water-based coating, the antibacterial microcapsules were added to the first topcoat, and the self-healing microcapsules to the second topcoat. Sample 9# (PT<sub>2a1s</sub>) was created through an independent adding method in which the primer was the water-based coating, the self-healing microcapsules were added to the first topcoat, and the antibacterial microcapsules were added to the second topcoat.

## 2.5. Testing and Characterization

### 2.5.1. Performance Characterization of Microcapsules

Encapsulation rate: First, 1.0 g of microcapsules was weighed and recorded as  $M_1$ . The microcapsules were then put in ethyl acetate for 72 h after thorough grinding. The amount of ethyl acetate should exceed that of the microcapsules. The remaining solution was rinsed and filtered repeatedly with distilled water in the vacuum filter (Shanghai Akuzann Scientific Instrument Co., Ltd., Shanghai, China). Then, the solution was dried in an oven at 60 °C. The remaining mass was recorded as  $M_2$ , and the coating rate,  $C$ , is as shown in Equation (1):

$$C = (M_1 - M_2)/M_1 \quad (1)$$

Based on the previous studies [30], nano-silver particles were almost impossible to observe due to their small content. So, the encapsulation rate of nano-silver solution microcapsules was 40%, and the core material containing nano-silver particles encapsulated in microcapsules was proved.

Microstructure and Chemical Composition: By using SEM (FEI Company, Hillsboro, OR, USA) and an optical microscope (OM, Carl Zeiss, Oberkochen, Germany), the microstructure of the self-healing microcapsules and coatings after scratching was observed. The chemical components of the microcapsules were analyzed by Fourier-transform infrared spectroscopy (FTIR, Germany BRUKER Co., Ltd., Karlsruhe, Germany) in the range of 4000–500  $\text{cm}^{-1}$ .

### 2.5.2. Gloss and Mechanical Properties

Color difference: Based on GB/T 11186.3-1989 [32], the color difference meter (Suzhou Weifu Photoelectric Technology Co., Ltd., Suzhou, China) was used to measure the color difference value of the coating. The coating without microcapsules was set as the control sample. According to Equation (2), the color difference value,  $\Delta E$ , was calculated, where  $L^*$  indicates the brightness of the coating,  $a^*$  indicates the red-green of the coating, and  $b^*$  indicates the yellow-blue of the coating.

$$\Delta E = [(\Delta L^*)^2 + (\Delta a^*)^2 + (\Delta b^*)^2]^{1/2} \quad (2)$$

Gloss: Based on GB/T 9754-2007 [33], samples were tested mainly with a 20°, 60°, and 85° angle of incidence. The gloss of the antibacterial coating prepared by antibacterial microcapsules was compared with that of the coating prepared without microcapsules. The higher the gloss, the better the appearance quality of the coating in general.

Coating transmittance: A UV spectrophotometer (Shanghai Smeo Analytical Instrument Co., Ltd., Shanghai, China) was used to test coatings applied to glass substrates. Coating transmittance was measured in the range from 300 nm to 800 nm. The visible band range was 600–800 nm. Coating transmittance values were calculated using Origin integration. The transparency of antibacterial coatings prepared with or without microcapsules was observed.

Hardness: Based on GB/T 6739-2006 [34], the coating's hardness was measured by pencils. The pencil hardness, 6 H-6 B, was used to rank the coating's hardness. The coating needed to be scratched under a load of 1.0 kg, and the pencils were kept at an angle of 45° under the tests. After the pencil with maximum hardness scratched the coatings, the coating was fractured. The pencil hardness with maximum hardness was recorded as the hardness value of the coatings.

Impact resistance: Based on GB/T 1732-2020 [35], the coating impact tester (Shenzhen sanuo Experimental Equipment Co., Ltd., Shenzhen, China) was used to test the impact resistance of the coatings. The impact force values were used to rank the deformation and damage of the coatings. Through the positioning height, a 1.0 kg weight hammer was released to produce an impact on the coatings. The coating was observed with a 4× magnifying glass to check for micro-cracks, wrinkles, and flaking. The maximum impact force values that did not cause damage to the coating were recorded as the impact resistance.

**Adhesion:** (1) Based on GB/T 4893.4-2013 [36], the coating's adhesion was chosen to be tested by the Baguette knife coating scribe (Hebei Zhongke Beigong Test Instrument Co., Ltd., Cangzhou, China). The blade was used to scratch the coating with force. The same process was used to scratch the coating at 90° vertically, forming a cross-cutting line. Afterwards, the grid lines were quickly attached with adhesive tape and removed to observe the peeling of the coatings. The adhesion rating was in descending order, from 0 to 5. No peeling occurred on the surface of the coating at grade 0. (2) Based on GB/T 5210-2006 [37], the adhesion tester (model BEVS 2201, Guangzhou Shenghua Co. Ltd., Guangzhou, China) was chosen to test the coating's adhesion. After the coating was dried, the test column was directly bonded to the coating, using an adhesive agent. After the adhesive agent was dried, the bonding test combination was placed on a suitable tensile testing instrument. The bonding test combination underwent a controllable pull-off test. The tensile force required to break the adhesion between the coating and substrate was measured.

**Roughness:** A JB-4C precision roughness meter (Shanghai Taiming Optical Instrument Co., Ltd., Shanghai, China) was selected to determine the coating's roughness, using contact measurements. The position of the Andoung wood was fixed. The coordinates were adjusted so that the probe touched the surface of the coating. The coordinate axis scale showed 0 when the test began. According to the measurement results, the average value was recorded as roughness. The unit of roughness (Ra) was  $\mu\text{m}$ .

**Tensile resistance:** The coating was applied to a glass board and dried before being removed. Then, the M-Testi universal mechanical testing machine (Changchun Xinte Testing Machine Co., Ltd., Changchun, China) was used to test the elongation at fracture of the coating. The elongation at fracture of the coating was calculated according to Equation (3), where  $L_0$  is the original length of the paint film,  $L$  is the length of the coating at the break, and  $e$  is the elongation at fracture of the coating. Based on the previous studies [38], as the elongation at fracture of the blank samples was 0%, it can be concluded that blank samples without self-healing microcapsules did not have the self-healing properties.

$$e = \frac{(L_0 - L)}{L} \times 100\% \quad (3)$$

**Resistance to liquid:** Based on GB/T 4893.1-2021 [39], the filter paper was wetted in liquid. Then, the filter paper was put on the coating. It was set aside for about 16–24 h. After that, the filter paper was taken away. The liquid was wiped off from the surface after 24 h. The samples were put under a light source to check the deterioration of coatings. The test areas were compared with the other areas, and the resistance to liquid of coatings was ranked according to the deterioration of coatings with the standard Table 5.

**Table 5.** Standard of the resistance to liquid of the coating.

Grade	Standard of Resistance to Liquid
1	The test area has no difference compared to that before the test.
2	Only when the light glowed, the coating reflected color, etc.
3	The color of the tested areas and the other areas was different according to different directions.
4	The coating was cracked or bulged.
5	The coating structure and color deteriorated, and the filter paper was stuck to the coating.

### 2.5.3. Antibacterial Properties of Coatings

**Strain preservation:** *Escherichia coli* and *Staphylococcus aureus* slant media were placed at 0–5 °C for strain preservation.

**Strain activation:** The required strains of bacteria were inoculated into the plate nutrient agar media. The constant-temperature and -humidity box (Shaoxing Shangcheng Instrument Co., Ltd., Shaoxing, China) was controlled at 36–38 °C and incubated for 18–20 h. A few fresh bacteria were scraped for 1–2 rings from the above inoculated media

with an inoculating ring, and were added to the nutrient broth. The concentration of the nutrient broth with bacteria required for the experiment was  $(5.0 - 10.0) \times 10^5$  cfu/mL (number of colonies per milliliter of sample).

Sample tests: According to GB/T 4789.2-2022 standard [40], the 0.4–0.5 mL nutrient broth with bacteria was moved by pipette and added dropwise on the blank control sample plate and antibacterial coating sample plate. A layer of sterilized plastic wrap was sealed on the sample plates by sterilized tweezers. There was no air bubble between the layer of plastic wrap and the coating. Then, the layer of plastic wrap was slowly pressed downward to make the suspension spread around. After that, the bacteria evenly contacted the sample. When finished, samples were transferred to a constant-temperature and -humidity box for incubation for 24 h. The temperature was formulated to 38 °C. The relative humidity (RH) was greater than 90%.

Preparation of plate nutrient agar media by dilution coating plate method: The wood surface and sealing plastic wrap were washed with 20 mL of eluent repeatedly. The eluent was added to the plate nutrient agar media. When the temperature was reduced to 45 °C, it was moved to plate nutrient agar media containing bacteria. After 48 h of incubation in a constant-temperature and -humidity box at 38 °C, colonies can be produced. Finally, the colony counter was used to count. The number of live bacteria measured above was multiplied by  $1 \times 10^3$ . The actual number of live bacteria recovered from each sample after 24 h of cultivation was observed. The antibacterial rate is calculated according to Equation (4).

$$R = (B - C)/B \quad (4)$$

where  $R$  = antibacterial rate, expressed in (%);  $B$  = number of bacteria recovered after 24 h of blank control sample plates (CFU); and  $C$  = number of bacteria recovered after 24 h of antibacterial coating sample plates (CFU).

The number of samples tested in the antibacterial experiment is denoted by  $N$ . In this test, the antibacterial test for one type of bacteria was performed 2 times. The standard deviation of the sample is denoted as  $S$  (Equation (5)), and  $X$  denotes the number of colonies measured in the sample.

$$S = \sqrt{\frac{1}{N-1} \sum_{i=1}^N (X_i - \bar{X})^2} \quad (5)$$

#### 2.5.4. Self-Healing Properties

By using a blade to scratch on the test samples, the width of the scratch was immediately observed under a microscope and labelled as  $H_0$ . After five days, the width of the scratch was again observed under a microscope and labelled as  $H_1$ . The self-healing rate is calculated according to Equation (6).

$$H = (H_0 - H_1)/H_0 \times 100\% \quad (6)$$

Four replications were completed for each sample. The test results show good reproducibility within a 5% error. A new sample was used for each test.

### 3. Results and Discussion

#### 3.1. Analysis of Microstructure and Chemical Composition of the Self-Healing Microcapsules

The FTIR of melamine–formaldehyde resin-coated rosin-modified shellac microcapsules are shown in Figure 1. The distinct vibrational peak at  $2980 \text{ cm}^{-1}$  was the  $-\text{CH}_2$  group, which was a rosin compound [41]. This indicates the presence of the core materials. The triazine ring absorption peak of the wall materials was at  $883 \text{ cm}^{-1}$ , the N-H stretching peak was at  $1558 \text{ cm}^{-1}$ , and the C-O peak appeared at  $1000 \text{ cm}^{-1}$ , thus indicating the presence of melamine–formaldehyde resin, the wall material. Thus, it can be proved that the melamine–formaldehyde resin-coated rosin-modified shellac microcapsules were successfully encapsulated.

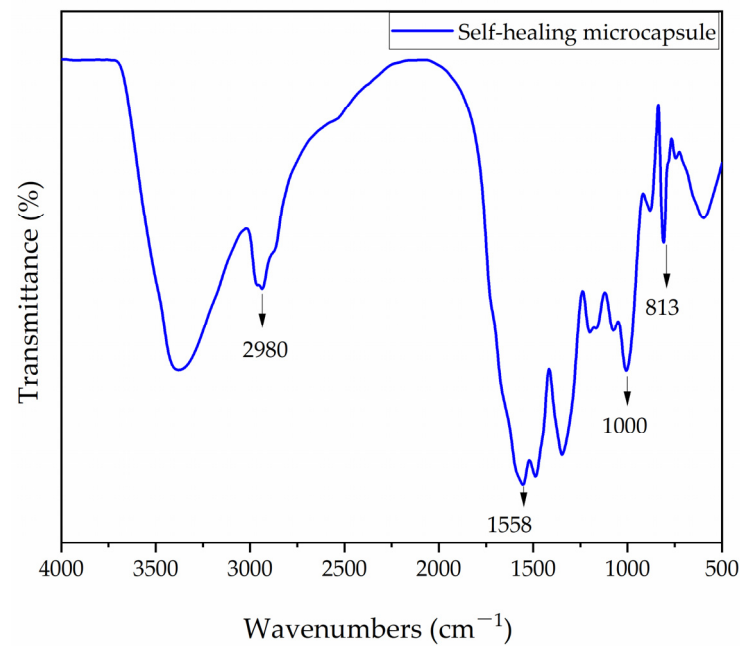


**Figure 1.** The FTIR of self-healing microcapsules.

SEM images of the self-healing microcapsules are shown in Figure 2. The microcapsule surface was smooth; there were many spherical microcapsules. This indicates that the self-healing microcapsules were successfully encapsulated.

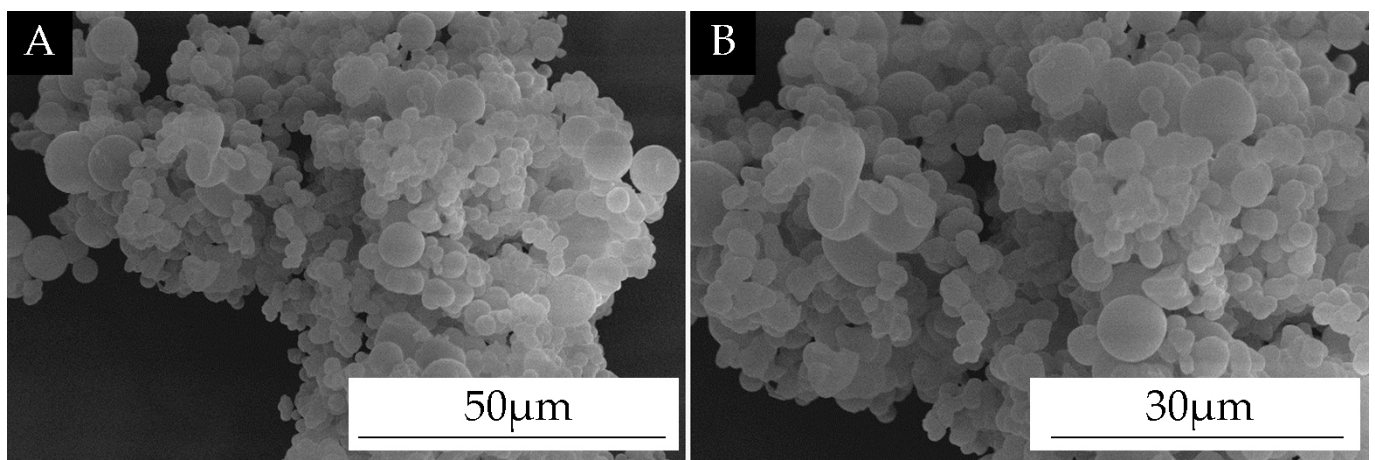


**Figure 2.** SEM of self-healing microcapsules. (A) low magnification; (B) high magnification.

### 3.2. Analysis of Orthogonal Test Results

According to the specific orthogonal test, the antibacterial rates were used as the results to test the range and variance, as shown in Table 6. The R-value of the adding method was obtained from the range results as 6.3, which was larger than that of the other two factors. The F of the adding method was obtained from the variance results as 1.825, which was larger than that of the other two factors.

Table 6. Analysis of range and variance.

Samples (#)	Content of Self-Healing Microcapsules (%)	Adding Method	Coating Method	Antibacterial Rate (%)
1	3	A	1 primer/2 topcoats	81.1
2	3	B	3 primers/2 topcoats	82.9
3	6	A	3 primers/2 topcoats	78.9
4	6	B	1 primer/2 topcoats	89.7
Mean value 1	82.0	80.0	85.4	
Mean value 2	84.3	86.3	80.9	
R-value	2.3	6.3	4.5	
SS	5.29	39.69	20.25	
d <sub>f</sub>	1	1	1	
F	0.243	1.825	0.931	
F <sub>crit</sub>	10.1	10.1	10.1	
Significance	-	-	-	

Figure 3 mainly shows the results obtained from the orthogonal test, where the six points represent the average antibacterial rate data of the four samples in pairs at each of the two levels and three factors. Figure 3 shows the effect of the three factors on antibacterial rates. The antibacterial rates of the coatings showed an increasing trend with the increasing content of the self-healing microcapsules. The antibacterial rates of the coatings were positively correlated with the adding methods and negatively correlated with the coating methods. The trend of antibacterial rates indicated that the biggest influencing factor was the adding methods of microcapsules. Therefore, combining the range and significance analysis, the preparation process to obtain the optimal antibacterial properties was that the adding method was B, the content of self-healing microcapsules was 6%, and the coating method was one primer and two topcoats.

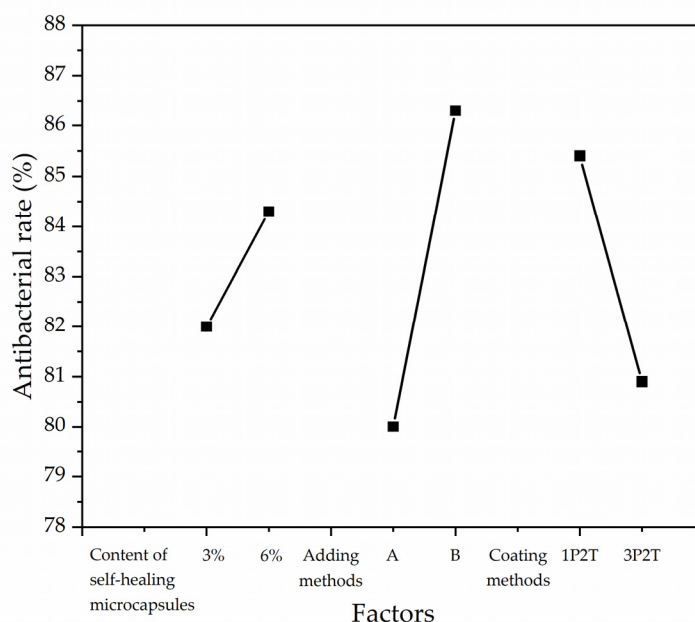


Figure 3. Effect of factors based on antibacterial rates.

### 3.3. Effect of Different Adding Methods on the Physical and Chemical Properties of Coatings

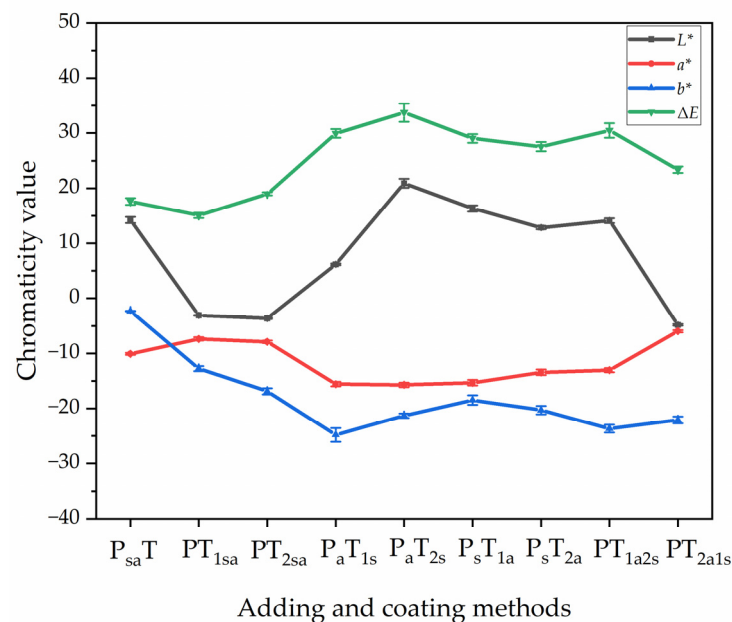
#### 3.3.1. Analysis of Color Difference and Gloss

Table 7 shows the color difference values of the coating on the Andoung wood obtained with different adding methods. The color difference was an important reference standard

for the optical properties of the coating. The coatings without microcapsules were used as the control samples. The chromaticity values for sample 0# showed an  $L^*$  value of 43.20,  $a^*$  value of 19.00, and  $b^*$  value of 29.30. The smaller the color difference values of the coating, the more the grain of the wood can be preserved. The  $\Delta E$  was the color difference value obtained by using the coating without microcapsules as the control sample. In samples 1#–3#, the color difference of the primer with microcapsules ( $P_{sa}T$ ) and the second topcoat with microcapsules ( $PT_{2sa}$ ) was 17.60 and 18.98, respectively. The adding of microcapsules to both the first and second topcoat resulted in a gradual increase in color difference due to an increase in the  $L$ . The highest color difference of 33.73 was obtained from sample 5# ( $P_aT_{2s}$ ) with adding method B. Figure 4 shows the trend of chromaticity values of the coatings. The values of the color difference of coatings prepared by the independent adding method B were higher than those of the coatings prepared by mixing adding method A. The higher value of the color difference indicates that the position where the microcapsules are located affects the overall color difference.

**Table 7.** Color difference values of coatings on the Andoung wood with different adding methods.

Samples (#)	Adding Methods	$L^*$	$a^*$	$b^*$	$\Delta L^*$	$\Delta a^*$	$\Delta b^*$	$\Delta E$
0	PT	43.20	19.00	29.30	0	0	0	0
1	$P_{sa}T$	59.53	8.91	26.98	14.23	−10.09	−2.32	17.60
2	$PT_{1sa}$	42.22	11.62	16.54	−3.08	−7.38	−12.76	15.06
3	$PT_{2sa}$	41.67	11.12	12.42	−3.63	−7.88	−16.88	18.98
4	$P_aT_{1s}$	51.48	3.42	4.50	6.18	−15.58	−24.80	29.93
5	$P_aT_{2s}$	66.20	3.30	7.98	20.90	−15.7	−21.32	33.73
6	$P_sT_{1a}$	61.64	3.67	10.83	16.34	−15.33	−18.47	29.04
7	$P_sT_{2a}$	59.42	5.95	5.62	12.85	−13.44	−20.30	27.53
8	$PT_{1a2s}$	58.15	5.56	9.00	14.12	−13.05	−23.68	30.50
9	$PT_{2a1s}$	40.47	13.02	7.23	−4.83	−5.98	−22.07	23.37



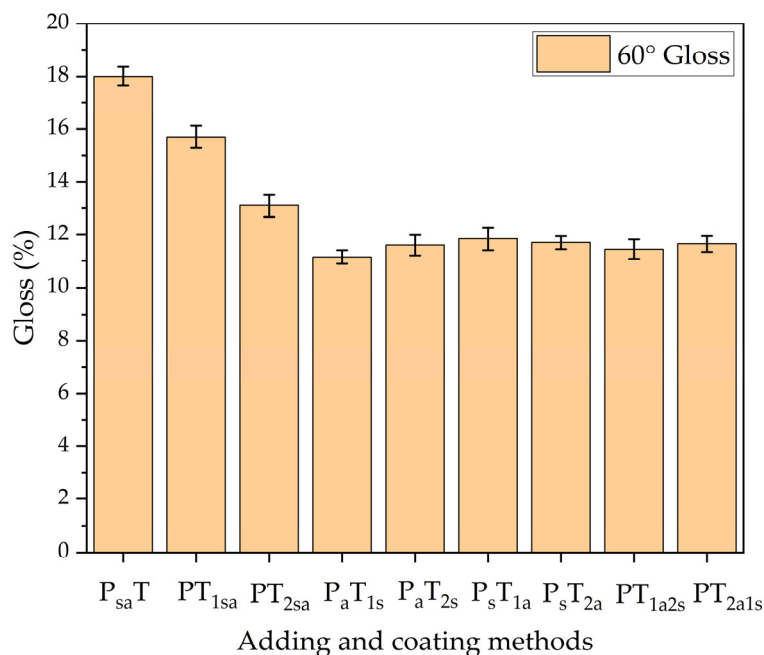
**Figure 4.** The trend of chromaticity values of the coating on the Andoung wood with different adding methods.

Table 8 shows the gloss grade of the coatings measured by different adding methods. The gloss grade was measured at a 60° angle of incidence, which was the main test value and can reflect the gloss of the coating. The better the gloss of the coating, the more it increases the surface color of the wood.

**Table 8.** Gloss of the surface coating of the Andoung wood with different adding methods.

Samples (#)	Adding Methods	Gloss (%)		
		20°	60°	85°
1	(A) P <sub>sa</sub> T	4.40	18.00	11.00
2	(A) PT <sub>1sa</sub>	4.40	15.70	10.50
3	(A) PT <sub>2sa</sub>	4.20	13.10	9.70
4	(B) P <sub>a</sub> T <sub>1s</sub>	2.10	11.15	8.40
5	(B) P <sub>a</sub> T <sub>2s</sub>	2.10	11.60	8.60
6	(B) P <sub>s</sub> T <sub>1a</sub>	2.10	11.85	9.20
7	(B) P <sub>s</sub> T <sub>2a</sub>	2.40	11.70	9.40
8	(B) PT <sub>1a2s</sub>	2.60	11.45	9.60
9	(B) PT <sub>2a1s</sub>	2.20	11.65	9.10

Figure 5 shows the trend of coating gloss with different adding methods. The gloss of sample 1# (P<sub>sa</sub>T) was 18%. The gloss of adding two types of microcapsules to the primer at the same time is better than that of adding them to the topcoat at the same time. The adding method B, in which the microcapsules were independently added to both the primer and topcoat reduced the coating gloss more. The self-healing microcapsules and antibacterial microcapsules were white and had different particle sizes, and when they were independently added to both the primer and the topcoat, the specular reflected light was weaker due to the unevenness of the surface. For the independent adding method B, the gloss of sample 6# (P<sub>s</sub>T<sub>1a</sub>) with the primer prepared by self-healing microcapsules and the topcoat prepared by antibacterial microcapsules was 11.85%. It was better than the adding method of the primer prepared by antibacterial microcapsules and topcoat prepared by antibacterial microcapsules. The content of microcapsules in the coating deteriorated the coating gloss and affected the color difference of the coating. It was necessary to refine the adding methods of microcapsules. The advantage of the independent adding method B was that the content of each microcapsule can be better controlled in order to achieve a more precise adjustment of the coating properties and obtain good optical properties.



**Figure 5.** The 60° gloss of coatings prepared by different adding methods.

### 3.3.2. Analysis of Mechanical Properties of Coatings

Figures 6 and 7 show the mechanical properties of the coatings on the Andoung wood, including hardness, adhesion, impact resistance, and roughness. Figure 6 shows the mechanical properties of coatings with different adding methods. The Andoung wood is borne to various mechanical stresses, such as friction and impact force, during actual use. Therefore, the coating on the wood plays a protective role. Figure 6A shows the coatings' hardness with different adding methods. The coating's hardness without microcapsules was up to 2 H, while the coating's hardness obtained by different adding methods was maintained at 3 H. This shows that the adding methods did not affect the coating's hardness. The content of microcapsules in water-based coatings increases the coating's hardness. Figure 6B shows the adhesion of coatings with different adding methods. From the results, we can see that the mixing adding method A and the independent adding method B that the primer prepared by antibacterial microcapsules made the coating's adhesion decrease.

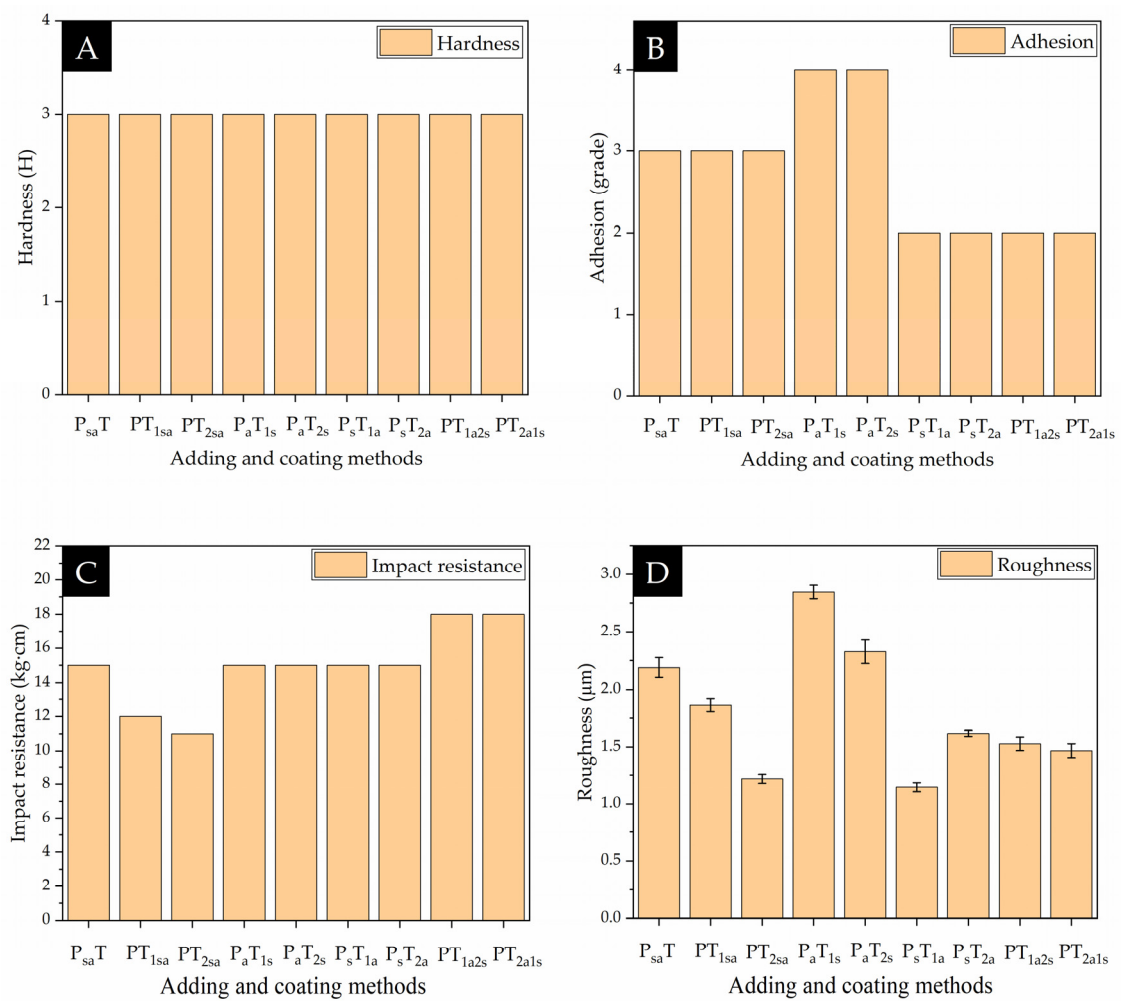


**Figure 6.** Mechanical properties of coatings with different adding methods. (A) hardness; (B) adhesion; (C) impact resistance; (D) roughness.

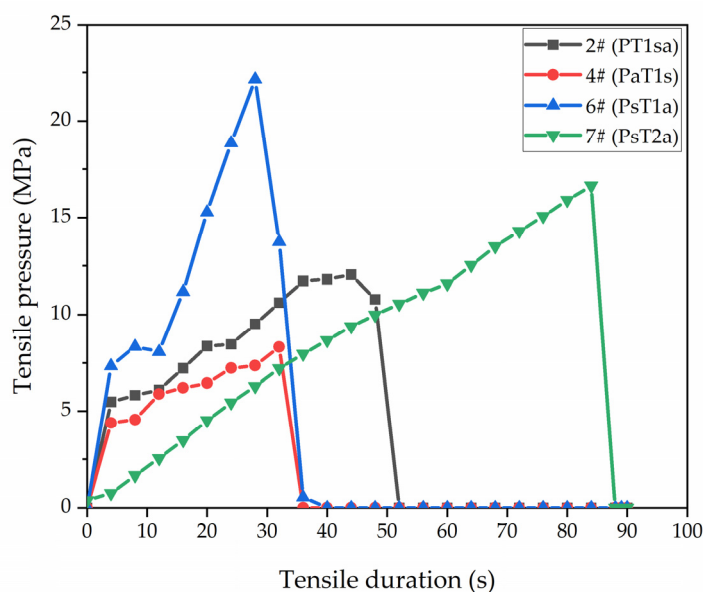


**Figure 7.** Adhesion between the coating and wood substrate by the pull-off tests.

Figure 6C shows the impact resistance of the coating with different adding methods. Under the mixed addition method, two types of microcapsules were mixed together, and the mechanical energy was converted into thermal energy when subjected to force. When the coating was prepared by independent adding method B, the microcapsules were in a state of high elasticity. When bore to the impact force, the microcapsules were able to absorb a larger amount of energy. Therefore, the impact resistance of sample 6# ( $P_sT_{1a}$ ) was up to 15 kg·cm. The antibacterial microcapsules can have good impact resistance no matter which topcoat they are added to.

As shown in Figure 6D, with the mixing adding method A, the microcapsules in the topcoat increased the coating's roughness. With the independent adding method B, sample 4# ( $P_aT_{1s}$ ) and sample 5# ( $P_aT_{2s}$ ) with the self-healing microcapsules in the different layers of the topcoat, independently, had a high overall roughness value of 2.85  $\mu\text{m}$  and 2.33  $\mu\text{m}$ , respectively. However, when the two types of microcapsules were added to the primer and topcoat, independently, the two types of microcapsules balanced the polymer molecules in the water-based coating. Therefore, the coating's roughness was reduced. Sample 6# ( $P_sT_{1a}$ ) had the lowest roughness of 1.144  $\mu\text{m}$ , while the coating was relatively flatted and smooth. Therefore, the independent addition method of using antibacterial microcapsules to prepare the topcoat and self-healing microcapsules to prepare the primer reduces the coating's roughness. The reason was that, when the microcapsules were added to the coating, the microcapsules effectively filled the defect of the coating, thus making the coating smoother and reducing the coating's roughness. At the same time, the microcapsules are also supported to form a protective coating, avoiding contact between the coating/wood substrate and the external environment. This reduced the influence of external factors on the coating and improved the durability and stability of the coating.

As shown in Figure 7, sample 2#, sample 4#, sample 6#, and sample 7# with the different adhesion levels were selected for the pull-off test. Through the comparison, we found that sample 6# bore the highest tensile pressure in a short time, which was significantly higher than that of sample 4#, which proved once again that adding antibacterial microcapsules to the primer independently reduced the coating's adhesion. Comparing sample 7# with sample 2# and sample 4#, sample 7# was better than sample 2# and sample 4# in terms of both the tensile pressure and inflection time, which indicated that adding self-healing microcapsules in the primer can increase the coating's adhesion. Sample 7# was better than sample 6# in terms of the inflection time, but the bearing tensile pressure was lower than that of sample 6#, thus indicating that the position of antibacterial microcapsules in the

topcoat affected the combining force in the coating. When the first topcoat was prepared with antibacterial microcapsules, the coating had higher adhesion, but the durability was poor. When the second topcoat was prepared with antibacterial microcapsules, there were better combining forces in the coating, as indicated by the higher durability. The content of antibacterial microcapsules reduced the completeness of the coating.

### 3.3.3. Analysis of Resistance to Liquids of Coating

The resistance to liquids of coatings refers to the properties of the coating in relation to its ability to maintain its original function and appearance under long-term or short-term exposure to various liquids. Wood products will be exposed to liquids such as water, acid, and beverages during use. That will cause the coating to turn white, lose light, bulge, or even crack. Therefore, the resistance to liquids of the coating is crucial. Table 9 shows the resistance to liquids of the coatings prepared by different adding methods. Whether it was the mixing adding method A or the independent adding method B, the coating left a red trace after resistance to red ink. The resistance to red ink was grade 5. The resistance to ethanol was grade 1 in all cases. The color of the detergent was transparent, so the change in the coating was not noticeable when the detergent was added dropwise to the coating's surface. The grade of detergent resistance of the coating without microcapsules was grade 2, which was observed by slight water stains on the coating. However, the grades of the resistance to liquids of the water-based coating with the microcapsules were improved. Under the same content of microcapsules, the coating prepared by mixing adding method A had a good grade 1 of resistance to liquids, whereas the resistance to liquids of the coating prepared by independent adding method B was worse. The coating released the nano-silver solution when the coating was borne to stress. The nano-silver solution was soluble in water easily and showed water stains when in contact with detergent, leaving a visible trace on the coating after the water evaporated. The density of the topcoat prepared with antibacterial microcapsules decreased. The defect of the coating was increased, causing liquids to penetrate it, thus reducing the grades of the resistance to liquids of the water-based coating.

**Table 9.** Resistance to liquids of coating on the Andoung wood with different adding methods.

Samples (#)	Add Methods	Resistance to Liquids (Grade)		
		Red Ink	Detergent	Ethanol
0	PT	5	2	1
1	(A) P <sub>sa</sub> T	5	1	1
2	(A) PT <sub>1sa</sub>	5	1	1
3	(A) PT <sub>2sa</sub>	5	1	1
4	(B) P <sub>a</sub> T <sub>1s</sub>	5	1	1
5	(B) P <sub>a</sub> T <sub>2s</sub>	5	2	1
6	(B) P <sub>s</sub> T <sub>1a</sub>	5	2	1
7	(B) P <sub>s</sub> T <sub>2a</sub>	5	2	1
8	(B) PT <sub>1a2s</sub>	5	2	1
9	(B) PT <sub>2a1s</sub>	5	2	1

### 3.3.4. Analysis of the Coating Transmittance

Figure 8 shows that different adding methods affected the coating transmittance in the wavelength range of 300–800 nm. The coating transmittance with different adding methods was calculated using Origin integration in the visible light interval at 800–600 nm. As shown in Table 10, the highest transmittance rate was 91.78% for sample 6# (P<sub>s</sub>T<sub>1a</sub>). The second highest transmittance rate was 91.38% for sample 1# (P<sub>sa</sub>T). In general, the overall coating transmittance of the independent adding method B was better than that of the mixing adding method A. However, the content of microcapsules of the topcoat negatively affected the coating transmittance. The main reason is that the microcapsules with the mixing adding method in water-based coatings had agglomerated. After drying, the

agglomeration increases the coating's roughness and leads to a diffuse reflection, resulting in a decrease in the coating transmittance.

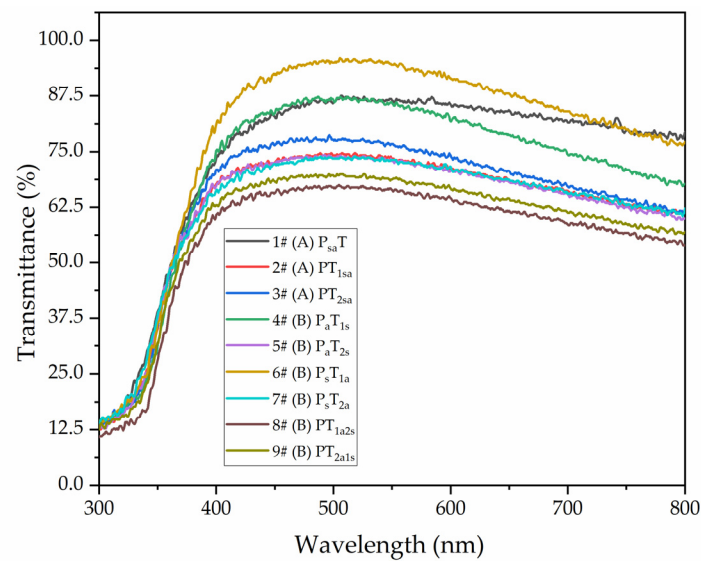


**Figure 8.** Coating transmittance with different adding methods.

**Table 10.** Visible light transmittance of coatings with different adding methods.

Samples (#)	Adding Methods	Visible Light Transmittance (%)
1	(A) P <sub>sa</sub> T	91.38
2	(A) PT <sub>1sa</sub>	88.07
3	(A) PT <sub>2sa</sub>	88.47
4	(B) P <sub>a</sub> T <sub>1s</sub>	88.07
5	(B) P <sub>a</sub> T <sub>2s</sub>	89.98
6	(B) P <sub>s</sub> T <sub>1a</sub>	91.78
7	(B) P <sub>s</sub> T <sub>2a</sub>	88.19
8	(B) PT <sub>1a2s</sub>	71.37
9	(B) PT <sub>2a1s</sub>	87.30

### 3.3.5. Analysis of Tensile Resistance of Coatings

The elongation at fracture of the coatings was measured before and after the scratching on coatings and after self-healing for 5 days, as shown in Table 11. Before scratching, the length of the water-based coating samples for testing was formulated to be 35 mm. The maximum elongation at fracture was taken as the tensile resistance. From the mixing adding method A, the mechanical properties of sample 1# (P<sub>sa</sub>T) were lower than that of sample 2# (PT<sub>1sa</sub>) and sample 3# (PT<sub>2sa</sub>). The elongation at fracture of sample 3# (PT<sub>2sa</sub>) reached 20.81%. With the independent adding method B, the highest elongation at fracture of 17.79% was achieved by sample 4# (P<sub>a</sub>T<sub>1s</sub>), in which the primer was prepared with antibacterial microcapsules and the topcoat was prepared with self-healing microcapsules. The elongation at fracture increased gradually because of the adding of self-healing microcapsules to the topcoat. The self-healing microcapsules in the topcoat, when borne to tensile force, fractured, and a small amount of the repairing agent flowed out, which increased the tensile resistance of the coating.

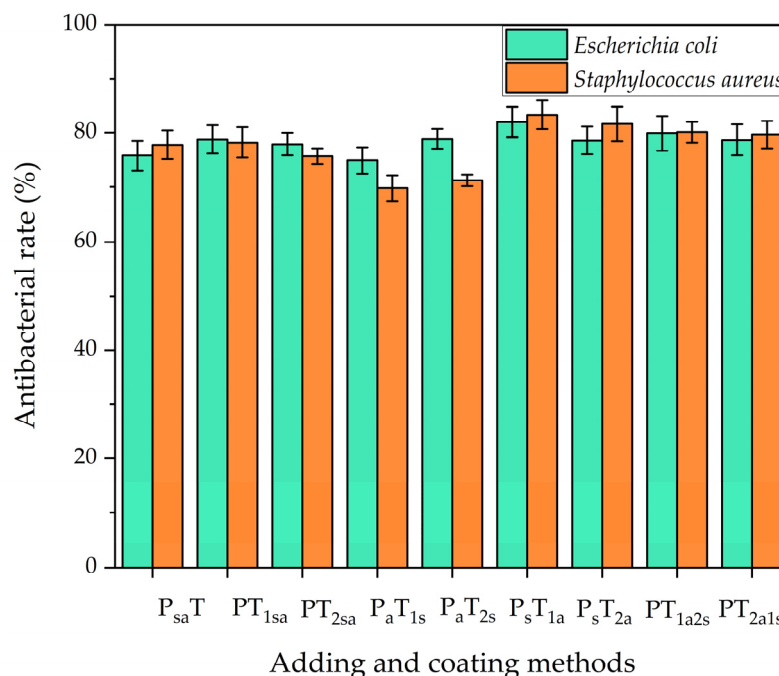
**Table 11.** Elongation at fracture with different adding methods in three conditions.

Samples (#)	Adding Methods	Elongation at Fracture (%)		
		Before Scratching	After Scratching	After Self-Healing
1	(A) P <sub>sa</sub> T	18.91	13.19	16.62
2	(A) PT <sub>1sa</sub>	19.78	14.92	17.38
3	(A) PT <sub>2sa</sub>	20.81	14.15	17.82
4	(B) P <sub>a</sub> T <sub>1s</sub>	17.79	14.46	16.12
5	(B) P <sub>a</sub> T <sub>2s</sub>	14.42	11.09	13.09
6	(B) P <sub>s</sub> T <sub>1a</sub>	17.86	14.52	16.72
7	(B) P <sub>s</sub> T <sub>2a</sub>	17.06	14.78	16.21
8	(B) PT <sub>1a2s</sub>	12.29	9.62	10.96
9	(B) PT <sub>2a1s</sub>	11.86	9.00	10.15

When the coating was measured again after self-healing for 5 days, the elongation at fracture was found to be much higher. The highest elongation at fracture, i.e., 17.82%, was achieved by sample 3# (PT<sub>2sa</sub>) with the mixing adding method A. For independent adding method B, the elongation at fracture of sample 6# (P<sub>s</sub>T<sub>1a</sub>) was 16.72%, which was an improvement of 2.2% over that after scratching. It showed that, when borne to tensile force, the self-healing microcapsules fractured so that the rosin-modified shellac would flow out, which repaired the coating and improved the mechanical properties of the coating.

### 3.4. Effect of Different Adding Methods on the Antibacterial Properties of the Coatings

Antibacterial tests were carried out against *Escherichia coli* and *Staphylococcus aureus*, respectively. The results are shown in Figure 9. It can be seen that the antibacterial coating prepared by both antibacterial microcapsules and self-healing microcapsules had almost the same antibacterial properties against *Escherichia coli* and *Staphylococcus aureus*.

**Figure 9.** Antibacterial properties of coatings on the Andoung wood.

With the mixing adding method A, when the two microcapsules were mixed by adding in the topcoat for sample 2# (PT<sub>1sa</sub>), the coating showed antibacterial rates against *Escherichia coli* and *Staphylococcus aureus* of 77.8% and 78.2%, respectively, which were superior to those of mixing adding in the primer. With the independent adding method B, the antibacterial rates of sample 4# (P<sub>a</sub>T<sub>1s</sub>) were only 74.9% and 69.8% against *Escherichia coli* and *Staphylococcus aureus*, respectively. Sample 5# (P<sub>a</sub>T<sub>2s</sub>) had a poor antibacterial effect, too. Sample 6# (P<sub>s</sub>T<sub>1a</sub>) had the highest antibacterial rates of 82% and 83.3% against *Escherichia coli* and *Staphylococcus aureus*, respectively. The antibacterial rates of sample 7# (P<sub>s</sub>T<sub>2a</sub>) were 78.6% and 81.7% against *Escherichia coli* and *Staphylococcus aureus*, respectively. The main difference between these two samples was the position of the antibacterial agent in the topcoat. The antibacterial rates of the independent adding method B were higher than those of the mixing adding method A. When the two types of microcapsules were mixed by adding, the agglomeration occurred, which deteriorated the properties of the microcapsules [42]. The coating with antibacterial microcapsules in the topcoat had the best antibacterial properties, mainly because the bacteria usually incubate on the surface of the coating. When the bacteria deteriorate the coating, the antibacterial microcapsules in the topcoat release a nano-silver solution to kill the bacteria.

### 3.5. Effect of Different Adding Methods on the Self-Healing Properties of Coatings

The effect of the adding methods on the self-healing properties of the coating on the Andoung wood was explored, as shown in Figure 10. Figure 10A shows the scratch of sample 1# measured under the microscope after scratching as 28.94  $\mu\text{m}$ . Figure 10B shows the scratch measured at the same location as Figure 10A after 5 days of self-healing. The scratch was 22.48  $\mu\text{m}$  after self-healing, which was narrowed by 6.46  $\mu\text{m}$ . The self-healing rate was calculated with Equation (6) as 22.3%. Figure 10C,D show the scratch narrowed by 2.79  $\mu\text{m}$  for sample 2#. Figure 10E,F show that the scratch narrowed by 5.59  $\mu\text{m}$  for sample 3#. Figure 10G,H show that the scratch narrowed by 0.35  $\mu\text{m}$  for sample 4#. Figure 10I,J show that the scratch narrowed by 1.57  $\mu\text{m}$  for sample 5#. Figure 10K,L show that the scratch narrowed by 6.86  $\mu\text{m}$  for sample 6#. Figure 10M,N show that the scratch narrowed by 4.85  $\mu\text{m}$  for sample 7#. Figure 10O,P show that the scratches narrowed by 1.95  $\mu\text{m}$  for sample 8#. Figure 10Q,R show that the scratches narrowed by 4.93  $\mu\text{m}$  for sample 9#.

As shown in Table 12, samples 1#–3# were prepared with the mixing adding method. The self-healing rates were 22.3%, 25.6%, and 24.3%, respectively. There was little difference in the self-healing properties. This indicates that mixing by adding antibacterial microcapsules in the topcoat did not affect the self-healing properties. When the antibacterial microcapsules were mixed and added to the primer, this method affected the self-healing properties of the self-healing coating. Samples 4#–9# were mainly prepared with the independent adding method. It was seen that the self-healing properties of sample 4# and sample 5# with the adding of self-healing microcapsules to the topcoat were poor, with only 2.6% and 7.6% self-healing rates. The self-healing rate of sample 6# with the adding of self-healing microcapsules to the primer reached 41.1%. The self-healing rate of sample 7# with nano-silver solution microcapsules added to the second topcoat and self-healing microcapsules added to the primer was 32.4%. The self-healing properties of sample 6# and sample 7# were better than those of the others. This indicates that the coating prepared with the method involving adding nano-silver solution microcapsules to the topcoat and self-healing microcapsules to the primer had the better self-healing properties. The reason is that, when micro-cracks occurred, the coating in contact with the wood was fractured by stresses, and the synergistic effect between the microcapsules was able to achieve good self-healing properties.

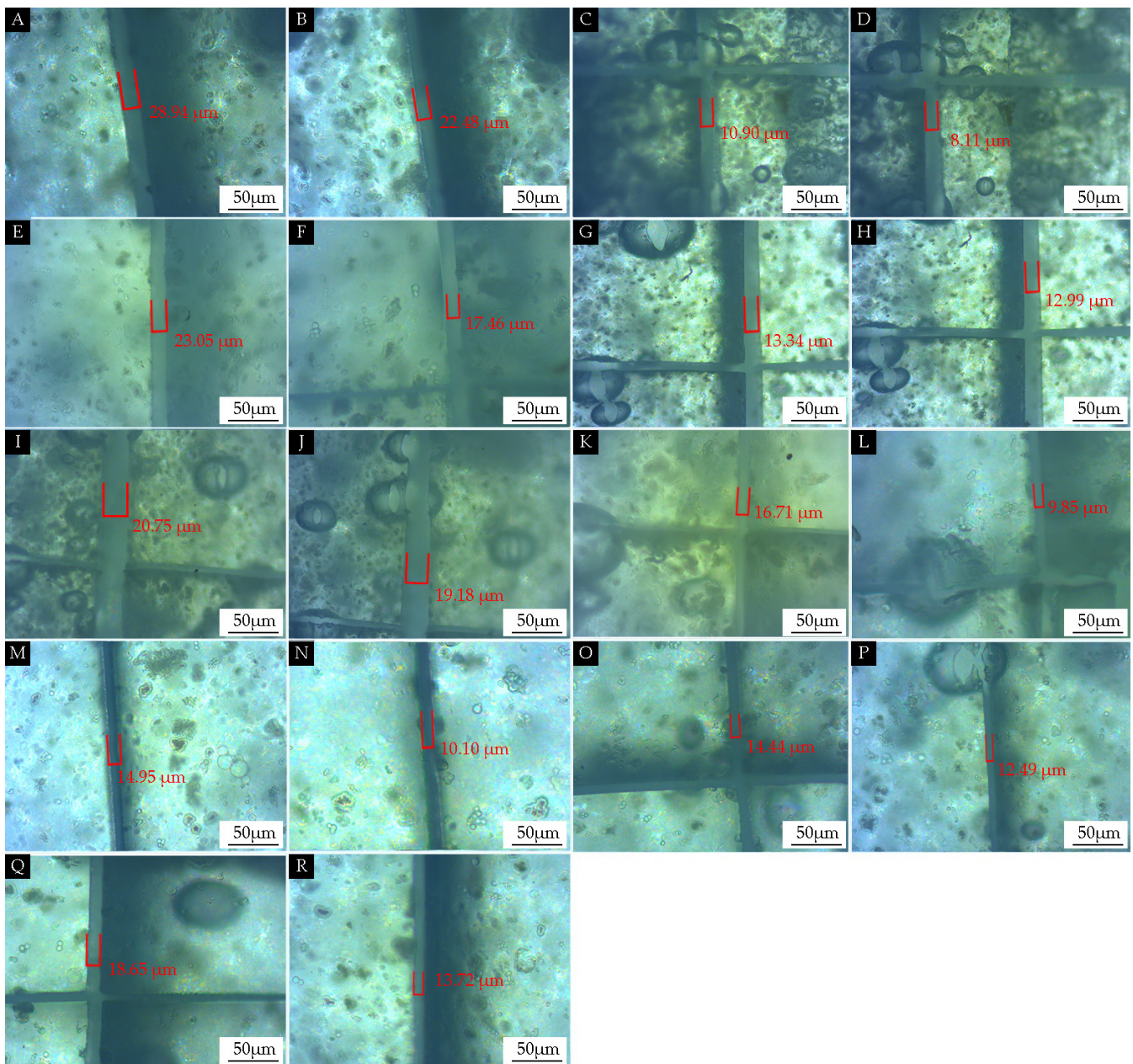


**Figure 10.** OM images of the self-healing properties of coatings with different adding methods: (A) after 1# scratch, (B) after 1# self-healing, (C) after 2# scratch, (D) after 2# self-healing, (E) after 3# scratch, (F) after 3# self-healing, (G) after 4# scratch, (H) after 4# self-healing, (I) after 5# scratch, (J) after 5# self-healing, (K) after 6# scratch, (L) after 6# self-healing, (M) after 7# scratch, (N) after 7# self-healing, (O) after 8# scratch, (P) after 8# self-healing, (Q) after 9# scratch, and (R) after 9# self-healing.

**Table 12.** Self-healing properties of the coating on the Andoung wood with different adding methods.

Samples (#)	Adding Methods	After Scratching ( $\mu\text{m}$ )	After Self-Healing ( $\mu\text{m}$ )	Self-Healing Rate (%)	Standard Deviation of Self-Healing Rate
1	(A) P <sub>sa</sub> T	28.94	22.48	22.30	0.0063
2	(A) PT <sub>1sa</sub>	10.90	8.11	25.60	0.0072
3	(A) PT <sub>2sa</sub>	23.05	17.46	24.30	0.0068
4	(B) P <sub>a</sub> T <sub>1s</sub>	13.34	12.99	2.60	0.0008
5	(B) P <sub>a</sub> T <sub>2s</sub>	20.75	19.18	7.60	0.0022
6	(B) P <sub>s</sub> T <sub>1a</sub>	16.71	9.85	41.10	0.0171
7	(B) P <sub>s</sub> T <sub>2a</sub>	14.95	10.10	32.40	0.0108
8	(B) PT <sub>1a2s</sub>	14.44	12.49	13.50	0.0041
9	(B) PT <sub>2a1s</sub>	18.65	13.72	26.40	0.0067

### 3.6. Self-Healing and Antibacterial Properties of Microcapsules in Coatings and Interfacial Interactions between Wood and Coating

#### (1) Comparison of antibacterial and self-healing properties of coatings

Taking sample 6# with optimal comprehensive performance as an example, the self-healing microcapsules were added to the primer, and the antibacterial microcapsules were added to the first topcoat. The coating's microstructure was analyzed by using SEM, as shown in Figure 11. Figure 11A shows an image of the coating's microstructure after scratching, and Figure 11B shows the image of that after the self-healing at the same position. It can be seen that the micro-crack of the coating was narrower after 5 days. This indicated that the core materials flowed out and filled the scratch.

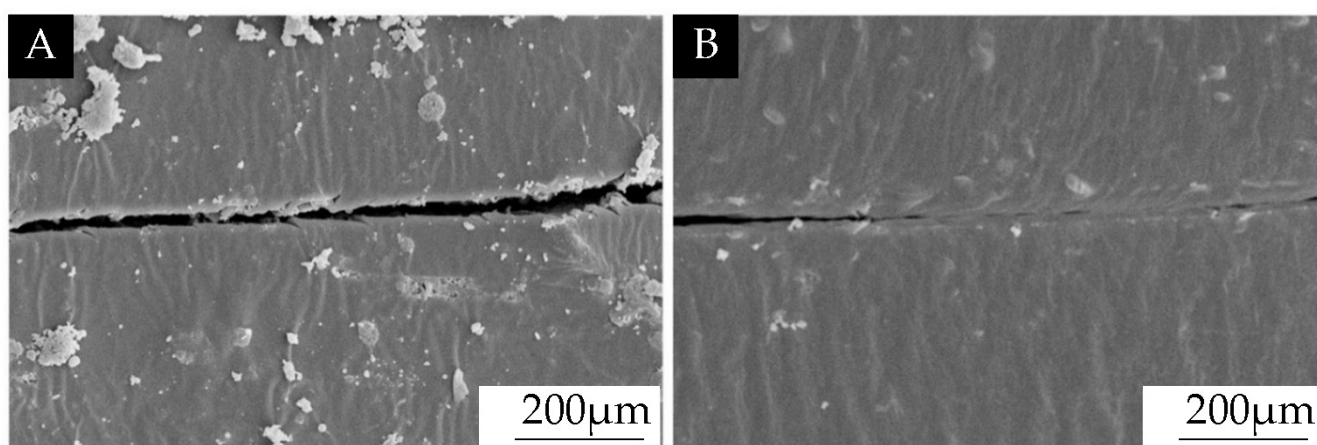


**Figure 11.** SEM images of the scratch of the coating prepared by antibacterial microcapsules and self-healing microcapsules: (A) after scratching on the coating and (B) after 5 days of self-healing.

#### (2) The mechanism analysis of antibacterial and self-healing properties of coatings

The mechanism analysis of the antibacterial and self-healing properties of coatings is shown in Figure 12. The scratch occurred on the coating after scratching. The microcapsules were borne to stresses, and the wall material was fractured and released the core materials. When the rosin-modified shellac came into contact with air, it was dried to fill the scratch of the coating at room temperature to achieve the self-healing [43,44]. Nano-silver particles, that is, the effective antibacterial component in the nano-silver solution, flowed out to form an antibacterial coating. The slow release of nano-silver particles from the antibacterial microcapsules caused the protein in the bacteria to coagulate to achieve the effect of bacterial inhibition. The nano-silver solution after encapsulation had better stability, a smaller size, and a stronger interaction with bacteria. At the same time, the microencapsulation technology protected the nano-silver particles from clustering, which

improved the antibacterial properties of the microcapsules [45]. The coating prepared by antibacterial microcapsules and self-healing microcapsules had significant antibacterial properties against *Escherichia coli* and *Staphylococcus aureus* and had significant self-healing properties to fill the micro-cracks.

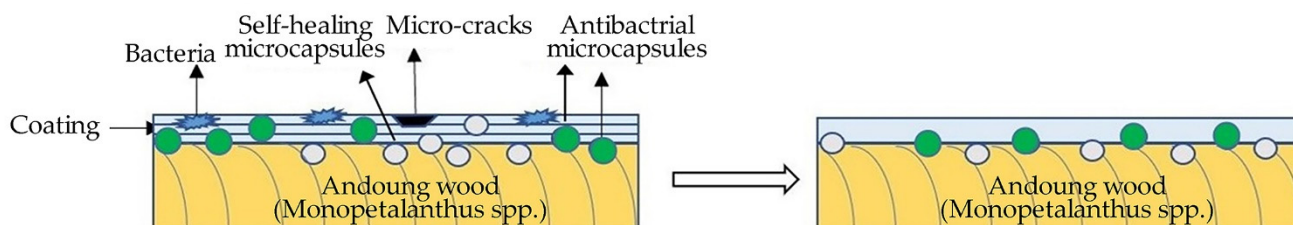


**Figure 12.** Antibacterial and self-healing mechanism of coatings on the Andoung wood.

#### 4. Conclusions

Dual-functional coatings prepared by mixing two microcapsules were investigated, including exploring the optical, mechanical, and resistance to the liquid properties of the coatings, as well as antibacterial and self-healing properties. The main influencing factor of the performance of the water-based coating was obtained as adding methods of antibacterial microcapsules and self-healing microcapsules. The gloss of the coatings with both antibacterial microcapsules and self-healing microcapsules added to the primer at the same time was superior to that of the one with both microcapsules added to the topcoat at the same time. The optimal coating gloss of sample 1# ( $P_{sa}T$ ) was 18%. Sample 6# ( $P_sT_{1a}$ ) had the optimal coating transmittance in the wavelength range of 300–800 nm of 91.78%. The coating's hardness was not affected by the adding method and was maintained at 3 H. The mechanical properties of coatings prepared with the independent adding method B were better than those of the mixing adding method A. The elongation at fracture of sample 6# ( $P_sT_{1a}$ ) after 5 days of self-healing was improved by 2.2% compared to that after scratching. The adding of self-healing microcapsules can improve the mechanical properties of the coating. Sample 2# ( $PT_{1sa}$ ) showed antibacterial properties against *Escherichia coli* of 77.8%, and *Staphylococcus aureus* of 78.2%, respectively. The mixing adding of microcapsules in the topcoat is better than that in the primer when comparing the antibacterial properties. With the independent adding method, the antibacterial rates of sample 6# ( $P_sT_{1a}$ ) reached 82% and 83.3%, respectively. Therefore, the antibacterial effect of the independent adding method B was superior to that of the mixing adding method A. Sample 6# ( $P_sT_{1a}$ ) had the optimal self-healing rate of 41.1%. The antibacterial microcapsules and self-healing microcapsules were added to the primer and topcoat in an independent method, which can develop their respective properties and effectively make coatings dual-functional. The dual-functional coatings provide the reference for preparing more functional and smarter coatings in the future.

**Author Contributions:** Conceptualization, methodology, validation, resources, data management, and supervision, Y.Z.; writing—review and editing, P.P. and N.Z.; formal analysis and investigation, X.Y. All authors have read and agreed to the published version of the manuscript.

**Funding:** This project was partly supported by the Natural Science Foundation of Jiangsu Province (BK20201386).

**Institutional Review Board Statement:** Not applicable.

**Informed Consent Statement:** Not applicable.

**Data Availability Statement:** Data are contained within the article.

**Conflicts of Interest:** The authors declare no conflict of interest.

## References

1. Zhou, C.; Huang, T.; Luo, X.; Kaner, J. Reorganisation and construction of an age-friendly smart recreational home system: Based on function–capability match methodology. *Appl. Sci.* **2023**, *13*, 9783. [CrossRef]
2. Hu, W.; Liu, N.; Xu, L.; Guan, H. Study on cold/warm sensation of materials used in desktop of furniture. *Wood Res.* **2020**, *65*, 497–506. [CrossRef]
3. Luo, Y.R.; Xu, W. Optimization of panel furniture plates rework based on intelligent manufacturing. *Bioresources* **2023**, *18*, 5198–5208. [CrossRef]
4. Luo, Z.Y.; Xu, W.; Wu, S.S. Performances of green velvet material (PLON) used in upholstered furniture. *Bioresources* **2023**, *18*, 5108–5119. [CrossRef]
5. Weng, M.Y.; Zhu, Y.T.; Mao, W.G.; Zhou, J.C.; Xu, W. Nano-silica/urea-formaldehyde resin-modified fast-growing lumber performance study. *Forests* **2023**, *14*, 1440. [CrossRef]
6. Hu, W.; Luo, M.; Liu, Y.; Xu, W.; Konukcu, A.C. Experimental and numerical studies on the mechanical properties and behaviors of a novel wood dowel reinforced dovetail joint. *Eng. Fail. Anal.* **2023**, *152*, 107440. [CrossRef]
7. Li, R.; Yao, Q.; Wang, X. Optimization of cutting power and power efficiency during particleboard helical milling. *Materialwiss. Werkstofftech.* **2023**, *54*, 158–167. [CrossRef]
8. Hu, W.; Wan, H. Comparative study on weathering durability properties of phenol formaldehyde resin modified sweetgum and southern pine specimens. *Maderas-Cienc. Tecnol.* **2022**, *24*, 17. [CrossRef]
9. Wang, C.; Zhang, C.Y.; Ding, K.Q.; Jiang, M.H. Immersion polishing post-treatment of PLA 3D printed formed parts on its surface and mechanical performance. *BioResources* **2023**, *18*, 7995–8006. [CrossRef]
10. Wang, C.; Zhou, Z. Optical properties and lampshade design applications of PLA 3D printing materials. *BioResources* **2023**, *18*, 1545–1553. [CrossRef]
11. Li, R.; He, C.; Xu, W.; Wang, X.A. Prediction of surface roughness of CO<sub>2</sub> laser modified poplar wood via response surface methodology. *Maderas-Cienc. Tecnol.* **2022**, *24*, 1–12. [CrossRef]
12. Bai, J.; Li, Y.; Jiang, S.S.; Guan, H.Y. Preparation of Wood Furniture Cooling Coatings Based on Phase Change Microcapsules and Its Performance Study. *Bioresource Technol.* **2022**, *17*, 1319–1337. [CrossRef]
13. Li, S.C.; Han, P.; Xu, H.P. Self-Healing Polymeric Materials. *Prog. Chem.* **2012**, *24*, 1346–1352.
14. Huh, A.J.; Kwon, Y.J. “Nanoantibiotics”: A new paradigm for treating infectious diseases using nanomaterials in the antibiotics resistant era. *J. Control. Release* **2011**, *156*, 128–145. [CrossRef]
15. Mittal, A.K.; Chisti, Y.; Banerjee, U.C. Synthesis of metallic nanoparticles using plant extracts. *Biotechnol. Adv.* **2013**, *31*, 346–356. [CrossRef] [PubMed]
16. Dhas, T.S.; Kumar, V.G.; Karthick, V.; Angel, K.J.; Govindaraju, K. Facile synthesis of silver chloride nanoparticles using marine alga and its antibacterial efficacy. *Spectrochim. Acta A* **2014**, *120*, 416–420. [CrossRef] [PubMed]
17. Husen, A.; Siddiqi, K.S. Phytosynthesis of nanoparticles: Concept, controversy and application. *Nanoscale Res. Lett.* **2014**, *9*, 229. [CrossRef]
18. Moyer, C.A.; Brentano, L.; Gravens, D.L.; Margraf, H.W.; Monafu, W.W., Jr. Treatment of Large Human Burns with 0.5 Per cent Silver Nitrate Solution. *Arch. Surg.* **1965**, *90*, 812–867. [CrossRef]
19. Gong, H.Y.; Solmaz, H.; Liu, W.F.; Ye, L. Imprinted polymer beads loaded with silver nanoparticles for antibacterial applications. *ACS Appl. Bio Mater.* **2021**, *4*, 2829–2838. [CrossRef]
20. Haidari, H.; Kopecki, Z.; Bright, R.; Cowin, A.J.; Garg, S.; Goswami, N.; Vasilev, K. Ultrasmall AgNP-impregnated biocompatible hydrogel with highly effective biofilm elimination properties. *ACS Appl. Mater. Interfaces* **2020**, *12*, 41011–41025. [CrossRef]
21. Huang, F.; Gao, Y.; Zhang, Y.M.; Cheng, T.J.; Ou, H.L.; Yang, L.J.; Liu, J.J.; Shi, L.Q.; Liu, J.F. Silver-decorated polymeric micelles combined with curcumin for enhanced antibacterial activity. *ACS Appl. Mater. Interfaces* **2017**, *9*, 16881–16890. [CrossRef]
22. Maryan, A.S.; Gorji, M. Synthesize of nano silver using cellulose or glucose as a reduction agent: The study of their antibacterial activity on polyurethan fibers. *Bulg. Chem. Commun.* **2016**, *48*, 151–155.
23. Nogueira, A.L.; Machado, R.A.F.; de Souza, A.Z.; Martinello, F.; Franco, C.V.; Dutra, G.B. Synthesis and characterization of silver nanoparticles produced with a bifunctional stabilizing agent. *Ind. Eng. Chem. Res.* **2014**, *53*, 3426–3434. [CrossRef]
24. Lakkim, V.; Reddy, M.C.; Pallavali, R.R.; Reddy, K.R.; Reddy, C.V.; Inamuddin; Bilgrami, A.L.; Lomada, D. Green Synthesis of Silver Nanoparticles and Evaluation of Their Antibacterial Activity against Multidrug-Resistant Bacteria and Wound Healing Efficacy Using a Murine Model. *Antibiotics* **2020**, *9*, 902. [CrossRef]
25. Abbas, A.; Amin, H.M.A.; Akhtar, M.; Hussain, M.A.; Batchelor-McAuley, C.; Compton, R.G. Eco-Friendly Polymer Succinate Capping on Silver Nano-Particles for Enhanced Stability: A UV-Vis and Electrochemical Particle Impact Study. *Chem. Naissensis* **2020**, *3*, 50–70. [CrossRef]
26. Brown, E.N.; Sottos, N.R.; White, S.R. Fracture testing of a self-healing polymer composite. *Exp. Mech.* **2002**, *42*, 372–379. [CrossRef]
27. Rodrigues, S.N.; Martins, I.M.; Fernandes, I.P.; Gomes, P.B.; Mata, V.G.; Barreiro, M.F.; Rodrigues, A.E. Scentfashion<sup>(R)</sup>: Microencapsulated perfumes for textile application. *Chem. Eng. J.* **2009**, *149*, 463–472. [CrossRef]
28. Xu, C.T.; Zeng, X.M.; Yang, Z.J.; Ji, H.B. Sunscreen Enhancement of Octyl Methoxycinnamate Microcapsules by Using Two Biopolymers as Wall Materials. *Polymers* **2021**, *13*, 886. [CrossRef] [PubMed]

29. Girard, J.; Brunetto, P.S.; Braissant, O.; Rajacic, Z.; Khanna, N.; Landmann, R.; Daniels, A.U.; Fromm, K.M. Development of a polystyrene sulfonate/silver nanocomposite with self-healing properties for biomaterial applications. *Cr. Chim.* **2013**, *16*, 550–556. [[CrossRef](#)]
30. Pan, P.; Yan, X.X. Preparation of Antibacterial Nanosilver Solution Microcapsules and Their Impact on the Performance of Andoung Wood Surface Coating. *Polymers* **2023**, *15*, 1722. [[CrossRef](#)] [[PubMed](#)]
31. Zou, Y.; Pan, P.; Yan, X. Comparative Analysis of Performance of Water-Based Coatings Prepared by Two Kinds of Anti-Bacterial Microcapsules and Nano-Silver Solution on the Surface of Andoung Wood. *Coatings* **2023**, *13*, 1518. [[CrossRef](#)]
32. GB/T 11186.3-1989; Methods for Measuring the Colour of Coating Films. Part III: Calculation of Colour Differences. Standardization Administration of the People's Republic of China: Beijing, China, 1990.
33. GB/T 9754-2007; Coatings and Varnishes-Determination of Specular Gloss of Non-Metallic Coating Films at 20°, 60° and 85°. Standardization Administration of the People's Republic of China: Beijing, China, 2007.
34. GB/T 6739-2006; Coating and Varnishes-Determination of Film Hardness by Pencil Test. Standardization Administration of the People's Republic of China: Beijing, China, 2006.
35. GB/T 1732-2020; Determination of Impact Resistance of Coating Films. Standardization Administration of the People's Republic of China: Beijing, China, 2020.
36. GB/T 4893.4-2013; Test of Surface Coatings of Furniture-Part 4: Determination of Adhesion-Cross Cut. Standardization Administration of the People's Republic of China: Beijing, China, 2013.
37. GB/T 5210-2006; Paints and Varnishes—Pull-Off Test for Adhesion. Standardization Administration of the People's Republic of China: Beijing, China, 2006.
38. Li, W.B.; Yan, X.X. Effects of Shellac Self-Repairing and Carbonyl Iron Powder Microcapsules on the Properties of Dulux Waterborne Coatings on Wood. *Polymers* **2023**, *15*, 2016. [[CrossRef](#)] [[PubMed](#)]
39. GB/T 4893.1-2021; Test of Surface Coatings of Furniture—Part 1: Determination of Surface Resistance to Cold Liquids. Standardization Administration of the People's Republic of China: Beijing, China, 2021.
40. GB/T 4789.2-2022; Microbiological Examination of Food Hygiene—Examination of the Residue of Antibiotics in Fresh Milk. Standardization Administration of the People's Republic of China: Beijing, China, 2022.
41. Bolcu, A.; Cioatera, N.; Bolcu, D.; Stanescu, M.M.; Ciuca, I.; Dinita, A.; Constantin, I. Chemical and Mechanical Properties for Rosin-Based Hybrid Resins. *Mater. Plast.* **2023**, *60*, 67–74. [[CrossRef](#)]
42. Kim, S.; Kim, J.H.; Ahn, K.H.; Lee, S.J. Rheological perspectives of industrial coating process. *Korea-Aust Rheol. J.* **2009**, *21*, 83–89.
43. Diesendruck, C.E.; Sottos, N.R.; Moore, J.S.; White, S.R. Biomimetic self-healing. *Angew. Chem. Int. Edit.* **2015**, *54*, 10428–10447. [[CrossRef](#)]
44. Bellan, L.M.; Pearsall, M.; Cropek, D.M.; Langer, R. A 3D Interconnected Microchannel Network Formed in Gelatin by Sacrificial Shellac Microfibers. *Adv. Mater.* **2012**, *24*, 5187–5191. [[CrossRef](#)] [[PubMed](#)]
45. Ferreira, A.M.; Vikulina, A.; Loughlin, M.; Volodkin, D. How Similar Is the Antibacterial Activity of Silver Nanoparticles Coated with Different Capping Agents? *RSC Adv.* **2023**, *13*, 10542–10555. [[CrossRef](#)] [[PubMed](#)]

**Disclaimer/Publisher's Note:** The statements, opinions and data contained in all publications are solely those of the individual author(s) and contributor(s) and not of MDPI and/or the editor(s). MDPI and/or the editor(s) disclaim responsibility for any injury to people or property resulting from any ideas, methods, instructions or products referred to in the content.